Electronic Supplementary Material (ESI) for Catalysis Science & Technology.
This journal is © The Royal Society of Chemistry 2018

Selectivity reversal of photocatalytic CO_2 reduction by Pt loading

Zhaoyu Ma,[a#] Penghui Li,[bc#] Liqun Ye*[ab] Li Wang,[a] Haiquan Xie,[a] and Ying Zhou*[b]

a Engineering Technology Research Center of Henan Province for Solar Catalysis, College of Chemistry and Pharmaceutical Engineering, Nanyang Normal University, Nanyang 473061, China.

b State Key Laboratory of Oil and Gas Reservoir Geology and Exploitation, Southwest Petroleum University, Chengdu 610500, China.

c Institute of Chemistry, National Institute of Measurement and Testing Technology, Chengdu 610021, China

[#] The authors contributed equally.

* Corresponding Author

E-mail: yeliquny@163.com (L. Ye); yzhou@swpu.edu.cn (Y. Zhou)

Synthesis

TiO_2: 10 ml tetrabutyl titanate and 1.2 ml hydrofluoric acid were mixed in a dried 50ml Teflon-lined stainless steel autoclave at 160 °C for 17h. The white product was filtrated and subsequently washedwith deionized water and ethanol , and dried at 60 °C overnight.

g-C_3N_4: Annealing urea at 550 °C for 4 hours with the heating rate of 5 °C min^{-1}.

BiOBr: 2 mmol $Bi(NO_3)_3•5H_2O$ and 2mmol KBr were dissolved in 40 ml absolute ethanol, and the solution was transferred to a 50 ml Teflon-lined stainless steel autoclave at 160 °C for 17 h. Finally, the precipitate was washed by centrifugation with distilled water and absolute ethanol, and dried at 60 °C for 24 h.

The methods of Pt loading on the surface of the catalyst by photo deposition are as follows: 500 mg TiO_2/ g-C_3N_4/ BiOBr are dispersed in 180 ml distilled water and 20 ml anhydrous methanol to followed by adding 1.5 ml of H_2PtCl_6. And then the mixture was stirred for 3 hours under 300 W xenon lamp (PLS-SXE300, Beijing Parker Light Source Technology Co., Ltd., China) irradiation . The resulting precipitate was filtered and washed with distilled water and anhydrous ethanol for several times, and dried at 60°C overnight.

Characterization

X-ray diffraction patterns (XRD) were recorde.d by Bruker D8 ADVANCE powder X-ray diffractometer (Bruker) with Cu Kα radiation generated at 40 kV and 30 mA. The 2θ range of XRD patterns were taken over 5–80°. Transmission electron microscopy (TEM) images were obtained by a JEOL JEM-2100F (UHR) Field Emission Electron Microscope working at 200 kV. X-ray photoelectron spectroscopy (XPS) was performed using Thermo ESCALAB 250XI X-ray photoelectron spectrometer (Al Ka, 150 W, C1s 284.8 eV). In situ infrared testing was performed on a Thermo Scientific Nicolet iS50 Fourier Transform Infrared (FT-IR) spectrometer (Thermo Fisher Scientific). Temperature programmed desorption (TPD) of CO gas was tested by Chemical adsorption instrument (AutoChem II 2920).

Photocatalytic CO_2 reduction

The photocatalytic CO_2 conversion was carried out under the condition of keeping the temperature constant in a closed system of Labsolar-III AG (Beijing Parkfrey Light Source Technology Co., Ltd., China). The volume of the reaction system was 350 ml. Firstly, 50 ml of distilled water was added to the bottom of the reactor and then 0.05 g of the catalyst was tiled on a circular flat glass measuring 28.26 square centimeters. The circular flat glass was then transfered to the reactor on a glass support. After that, the vacuum grease was uniformly applied to seal the above the reactor. The CO_2 gas is filled inside the reactor before light irradiation，then at a distance of 10 cm just above the reactor, a 300 W high pressure xenon lamp (PLS-SXE300, Beijing Parker Light Source Technology Co., Ltd., China) was irradiated and a DC-0506 cryostat Instrument Co., Ltd., China) maintains a light reaction temperature of 20°C. During the irradiation, 1 ml of gas was withdrawn from the reactor every half an hour and injected into a GC9790 II gas chromatograph equipped with a flame ionization detector (FID, GDX-01 packed column) (Zhejiang Foli Analysis Instrument Co., Ltd., China). The gases exported are identified as CO, CO_2, and CH_4.and the amount of product is calibrated using the calibration curve.

In-situ DRIFTS measurement

During the in-situ DRIFTS measurement, the sample was filled into the in-situ IR cell, and CO_2 and H_2O gases were introduced into the cell and LED monochromatic light of 365 nm irradiated on the sample through the CaF2 window of the cell. Before the measurement, the sample was degassed at high temperature for 1 hour in a Vacuum drying oven. The baseline was obtained after adsorption equilibrium of CO_2 on the sample for 1 h.

Density functional theory (DFT) calculations method

Our Density functional theory (DFT) computations were carried out by using an all-electron method within a generalized gradient approximation (GGA) for the exchange-correlation term, as implemented in the DMol^3 code. The double numerical plus polarization (DNP) basis set and Perdew-Burke-Ernzerhof (PBE) exchange-correlation functional were adopted. A convergence criterion of 10^{-6} a.u.

were performed with the total energy and electron density in self-consistent field (SCF) computations. To ensure high-quality numerical results, we chose the real-space global orbital cutoff radius as high as 4.6 Å in all computations. The Brillouin zones of Pt clusters were sampled with 3× 3 × 1 *k* points d in reciprocal space during geometry optimization. To know about the adsorption stability of these main products (CO_2, CO, CH_4), the adsorption energy have been as following formula:

$$E_{ads} = E_{total} - E_{Pt} - E_{molecule}$$

Where E_{total} denotes the total energy of Pt clusters with molecules. E_{Pt} and $E_{molecule}$ are the energy of bare Pt clusters and single molecule in gas phase, respectively.

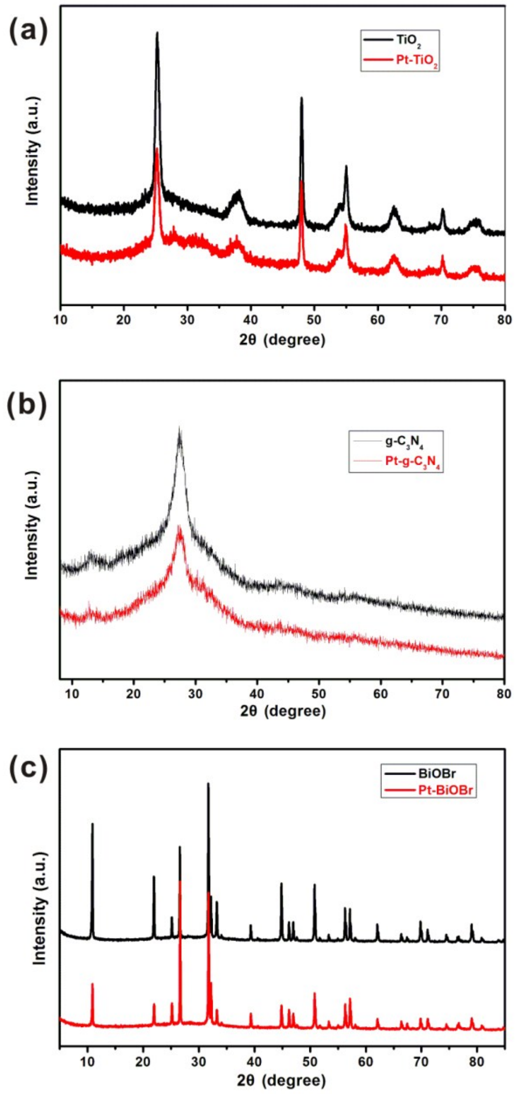

Figure S1. X-ray diffraction pattern of (a) TiO_2 and Pt-TiO_2, (b) g-C_3N_4 and Pt-g-C_3N_4, and (c) BiOBr and Pt-BiOBr.

Figure S1 showed the powder X-ray diffraction pattern of three photocatalyst. After loading noble metal Pt on the surface of catalyst, the peak position did not change. But some peak intensity weakened after Pt loading. No characteristic peak of Pt was seen on the three kinds of photocatalysts due to the low amount.

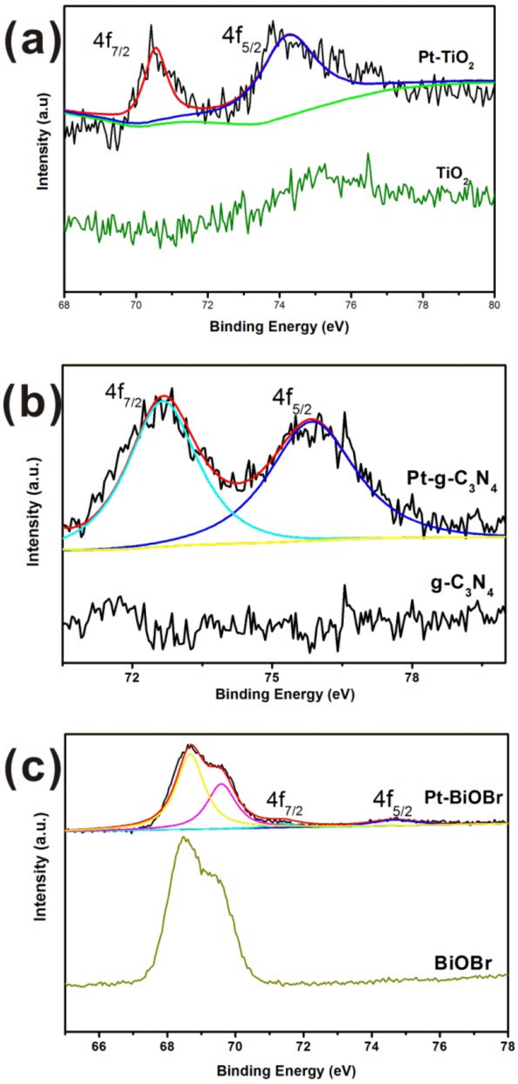

Figure S2. X-ray photoelectron spectroscopy pattern

The chemical state of the surface Pt nanoparticles was characterized by high resolution Pt 4f XPS (X-ray photoelectron spectroscopy), and the calibration on the Pt 4f XPS spectra was based on the standard binding energy of C (sp^2) at 284.6 eV. It can be seen in Figure S2 that the signal of the Pt 4f peak is detected on the surface of the three photocatalysts, indicating that the Pt nanoparticles on the photocatalyst surface are successfully loaded. The shift of the peak to high binding energy can be used as evidence of the interaction between Pt and photocatalyst. According to the position, it can be seen that the Pt nanoparticles on the surface of the photocatalyst are metal Pt.

(1) W. Guo, Q. Qin, L. Geng, D. Wang, Y. Guo. Y. Yang, Morphology-Controlled

Preparation and Plasmon-Enhanced Photocatalytic Activity of Pt-Biobr Heterostructures. J Hazard Mater. 2016, 308, 374-85.

(2) S. Liang, Y. Xia, S. Zhu, S. Zheng, Y. He, J. Bi, M. Liu. L, Wu. Au and Pt Co-Loaded G-C_3N_4 Nanosheets for Enhanced Photocatalytic Hydrogen Production under Visible Light Irradiation. Applied Surface Science. 2015, 358, 304-312.

(3) Y. Wang, J. Zhao, Y. Li, C. Wang, Selective photocatalytic CO_2 reduction to CH_4 over Pt/In_2O_3: Significant role of hydrogen adatom, Applied Catalysis B: Environmental. 2018, 226, 544-553.

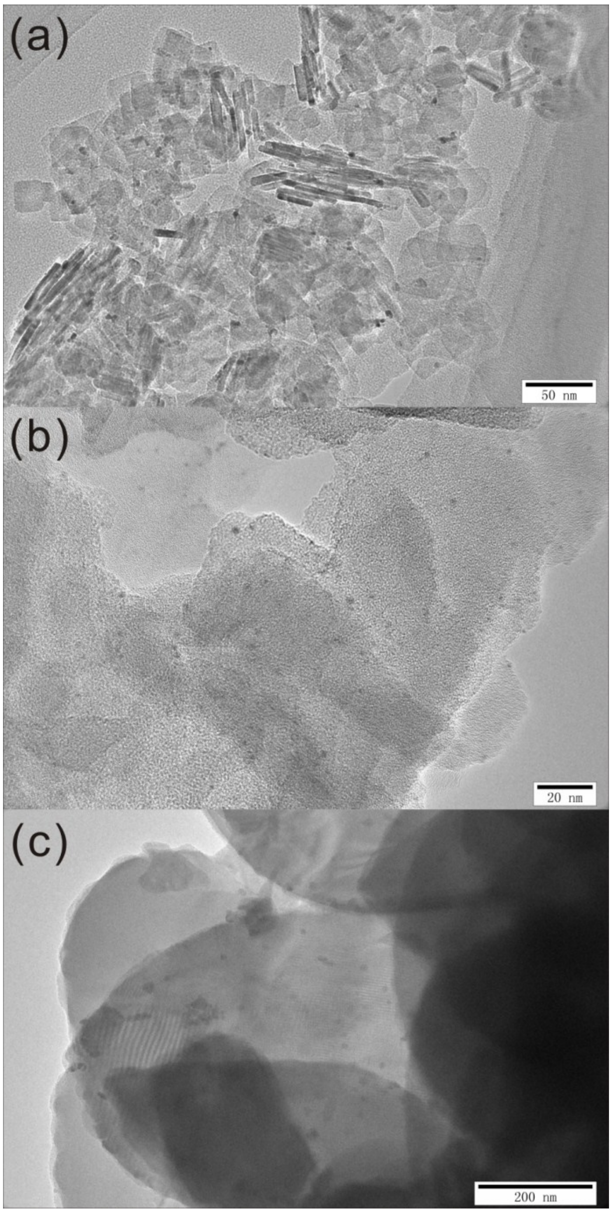

Figure S3. TEM of Pt-TiO_2 (a), Pt-g-C_3N_4 (b) and Pt-BiOBr (c).

Figure S3 is transmission electron microscopy (TEM) images of three photocatalysts. It can be seen in the TEM images that Pt particles are successfully loaded on the surface of the catalyst and have a uniform distribution.

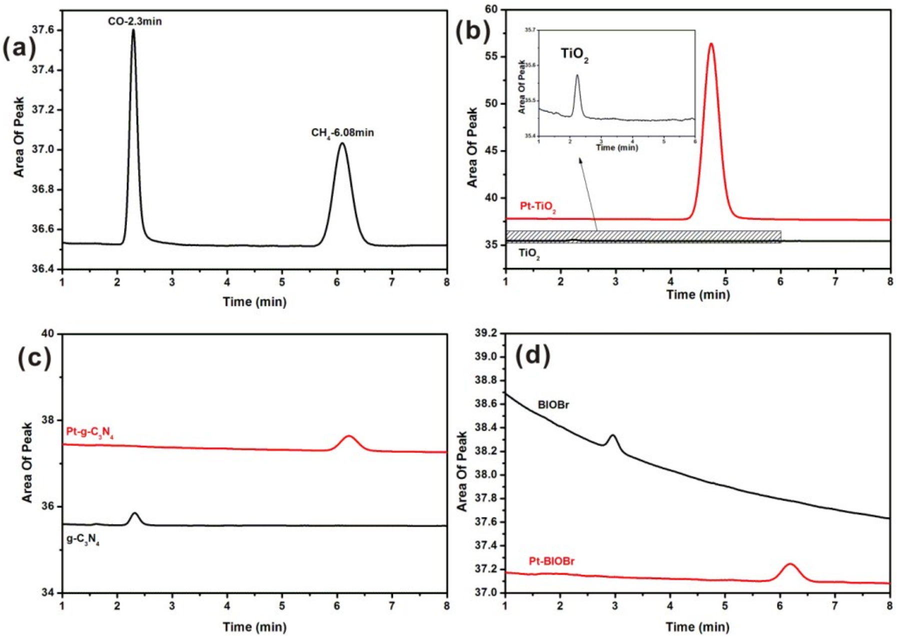

Figure S4. GC spectrum: (a) standard for CO and CH_4, (b) TiO_2 and Pt-TiO_2, (c) g-C_3N_4 and Pt-g-C_3N_4, (d) BiOBr and Pt-BiOBr.

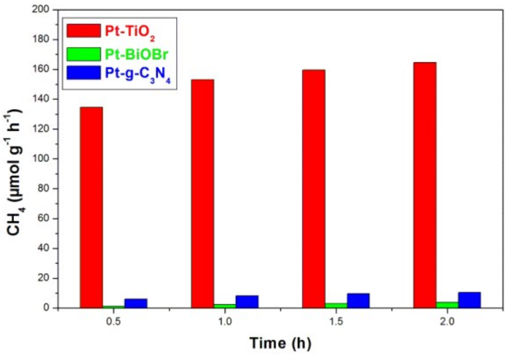

Figure S5. Photocatalytic CO_2 reduction over Pt-TiO_2, Pt-g-C_3N_4, and Pt-BiOBr.

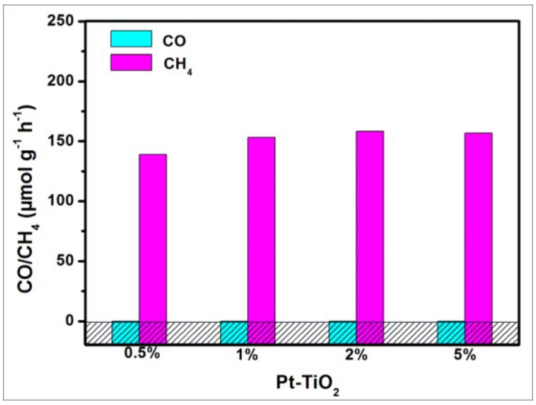

Figure S6.Effect of the amount of Pt loadings on TiO_2 for CO_2 reduction.

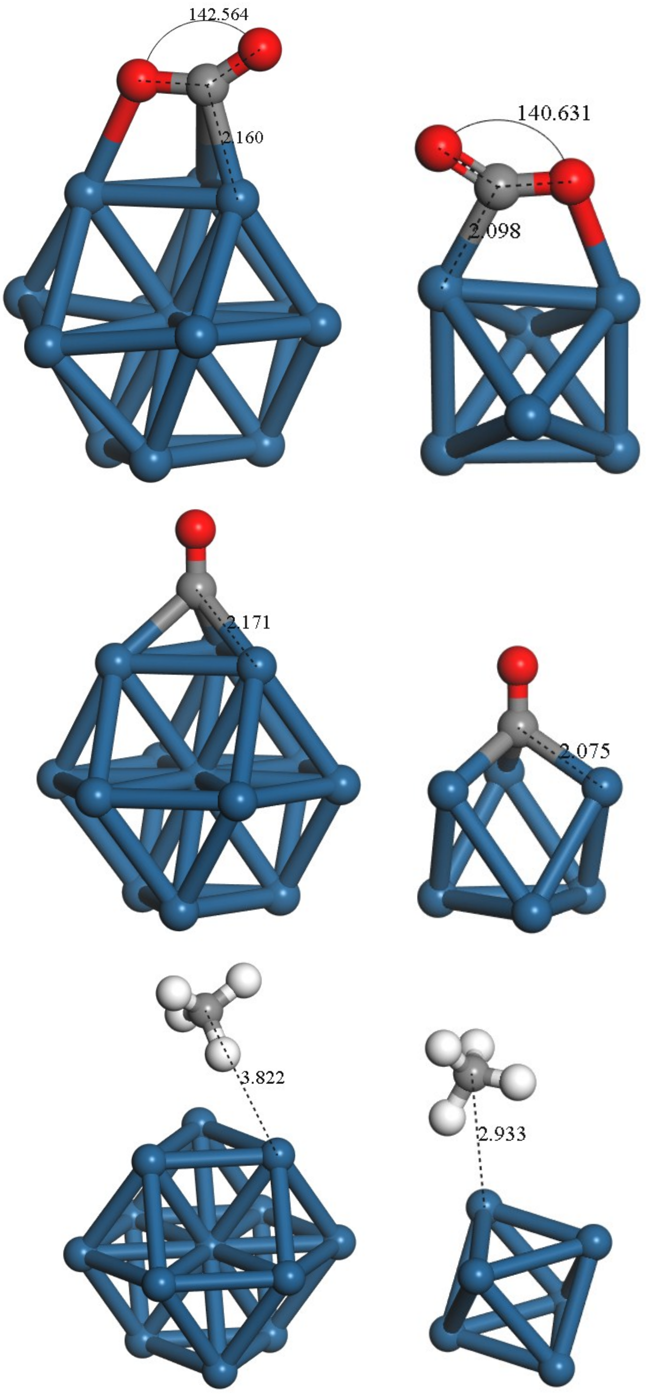

Pt13 (3Å) Pt6 (2Å)

Figure S7. Pt models of different particle sizes, Pt13 (3Å) and Pt6 (2Å).

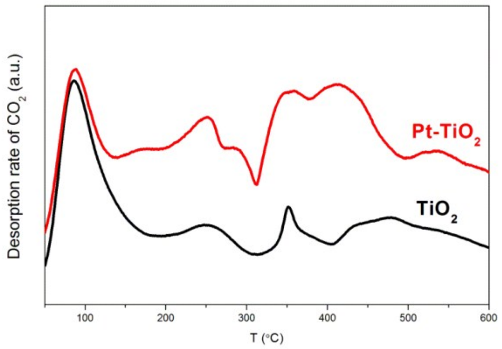

Figure S8 CO-TPD of TiO_2 and 1%Pt/TiO_2.

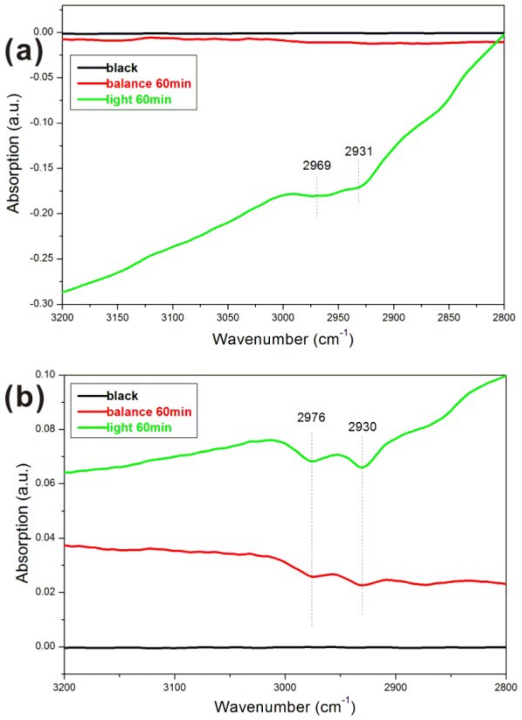

Figure S9 In-situ DRIFT spectra of CO_2 and H_2O reaction on (a) TiO_2 and (b) 1%Pt/TiO_2.